

Interferometric Study of Unsteady Convective Motion of Liquids

Yuko Oshima (大島 裕子)

Department of Physics, Faculty of Science,
Ochanomizu University, Tokyo

(Received April 11, 1966)

Introduction

When a finite amount of heat energy is released at a point in a uniform fluid at rest, a part of fluid begins to move upward due to the buoyancy force. This buoyant fluid, which is called "thermal", ascends vertically and eventually diffuses away into ambient fluid. At the first stage of its development, a warm spherical body of fluid is created around the heat source; in the next stage, it grows larger and moves upward preserving its spherical shape unchanged; and finally it deforms to a mushroom shape and diffuses away.

This kind of phenomena, unsteady free convection flow, has been studied mostly by meteorologists, e.g., Scorer¹⁾, Turner^{2,3)}, Woodward⁴⁾ etc. in connection with the development of the cumulus clouds. Morton⁵⁾ tried to analyse the early stage of these unsteady convective motion. The complete theory has not yet been presented, and the detailed observations in the laboratory experiments for verifying theory are rather scanty.

Recently the author investigated the problem of free convection and examined its self-similar solution and further compared it with the observations in the water and glycerin⁶⁾. In these experiments, a double refraction interferometer was used in order to determine the position of the center of the buoyant mass of fluid. In this report, the temperature distributions in the heated core will be presented, which are measured by Mach-Zehnder interferometry. For this purpose we used a He-Ne gas laser for the light source of the interferometer which made the adjustments of the interferometer extremely easy owing to its excellent brightness and coherency.

Analysis

The general analysis of the free convective motion is described in the former report⁶⁾. Here it is briefly summarized.

The basic equations of this problem are the equations of conservation of mass, momentum and energy. They are

$$\operatorname{div} \mathbf{v} = 0,$$

$$\frac{\partial \mathbf{v}}{\partial t} + (\mathbf{v} \cdot \operatorname{grad}) \mathbf{v} = \mathbf{B}\theta - \frac{1}{\rho} \operatorname{grad} p + \nu \nabla^2 \mathbf{v},$$

$$\frac{\partial \theta}{\partial t} + (\mathbf{v} \cdot \operatorname{grad}) \theta = \kappa \nabla^2 \theta,$$

respectively, where \mathbf{v} is the velocity of the fluid, p is the pressure, θ is the temperature increase over that of the undisturbed region, and t is the time, ρ , ν and κ are the density, the kinematic viscosity and the thermal diffusivity of the fluid, respectively. The buoyancy factor \mathbf{B} is the product of the thermal expansion coefficient β and the acceleration of the gravity \mathbf{g} i. e. $\mathbf{B} = -\beta \mathbf{g}$. The temperature difference θ is assumed to be so small that all the physical properties of the fluid are independent of the expected temperature variation. Since the velocity of the convective flow is also small, the viscous dissipation term in the energy equation may be neglected. Then the total heat quantity corresponding to the excess temperature all over the fluid at any time is the same as the heat energy Q released at the point source instantaneously.

$$Q = \rho c_p \iiint_{-\infty}^{\infty} \theta dx dy dz = \rho c_p Q'.$$

For the four parameters Q' , κ , ν and B , which relate to this problem, two non-dimensional parameters, the Prandtl number σ and the Grashof number G are defined as

$$\sigma = \frac{\nu}{\kappa},$$

$$G = \frac{BQ'}{\rho c_p \nu^2}.$$

We can make all the variables non-dimensional by use of a characteristic length $h = \sqrt{\kappa t}$ as follows

$$x = hX, \quad y = hY, \quad z = hZ$$

$$u = \frac{2\kappa}{h} U, \quad v = \frac{2\kappa}{h} V, \quad w = \frac{2\kappa}{h} W,$$

$$\theta = \frac{Q}{\rho c_p} \frac{\Theta}{h^3},$$

where x, y, z, u, v, w and θ are the Cartesian coordinates of the system, the velocity components in each direction of the coordinate axes and

the temperature excess over the undisturbed medium, respectively. Here the quantities in the capital letters are the non-dimensional expression corresponding to those in the small letters, respectively. The self-similarity in this case implies that these non-dimensional variables are functions of σ and G only, and it has been confirmed as regards buoyant motion in the previous paper. More precisely, if temperature excesses are small, we can predict analytically that the non-dimensional height of the highest temperature point Z_0 shall be proportional to G , and the ratio of Z_0 to G shall be function of σ only. These conjectures were remarkably established by the experiments reported in the previous paper as shown in the Figs. 1 and 2.

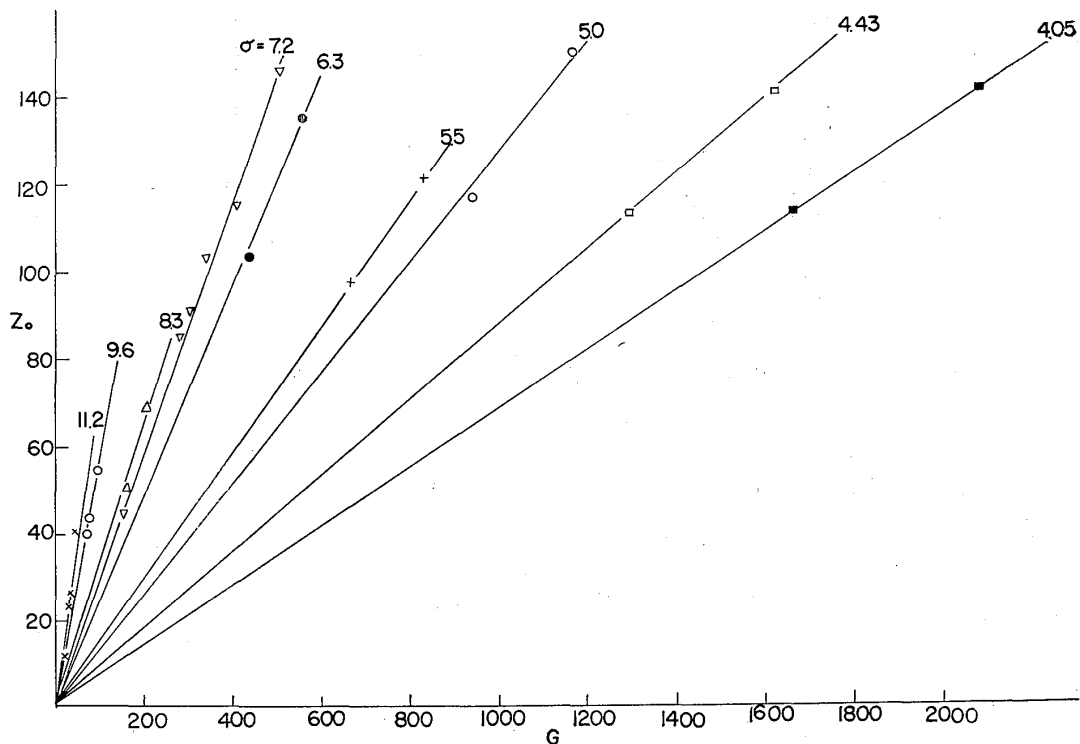


Fig. 1. The relation between Z_0 and G in water

In the same way, it is ascertained that there exists the self-similarity in the temperature distribution, and especially at earlier stages of the convective motion it is expressed as

$$\Theta = \frac{1}{\pi^{3/2}} e^{-R^2},$$

where R is the non-dimensional radial distance measured from the center of the buoyant mass at each time⁶⁾.

The temperature excess θ at a point in the flow field is determined by the fringe shift in the interferogram. In these experiments θ is not so large that ϵ is proportional to θ : $\theta = K\epsilon$, where K is a factor composed of the sensitivity of interferometer, thermal expansion

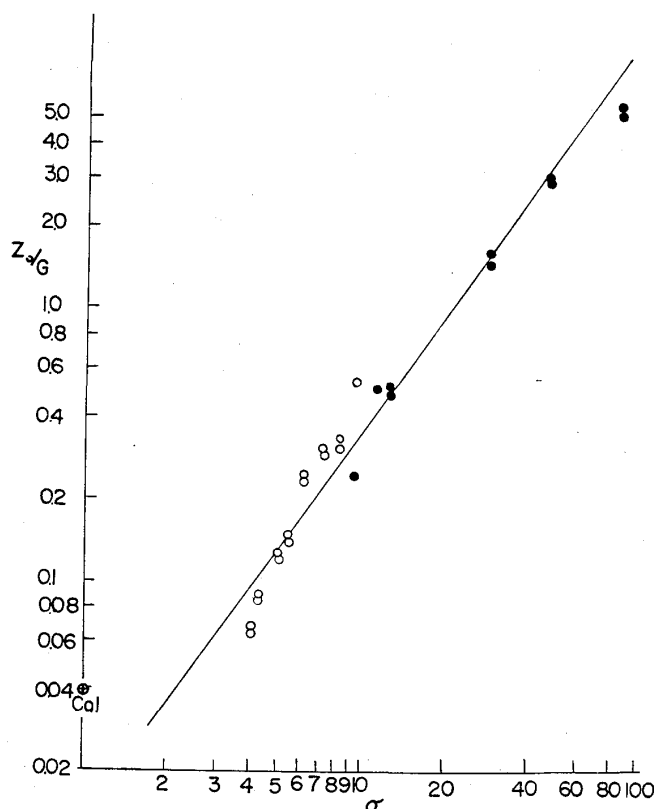


Fig. 2. The relation between Z_0/G to σ , \circ is water, \bullet is mixture of glycerin and water.

coefficient of fluids, magnifications of photographs etc., and of common value throughout the present experiments. If the above mentioned self-similarity exists, θ or ε varies as h^{-3} or $(\kappa t)^{-3/2}$. Then the relation between $\varepsilon t^{3/2}$ and x/\sqrt{t} or z/\sqrt{t} shall remain unchanged in a run of one experiment. Further, if ε is transformed into the non-dimensional variable $\Theta = K\varepsilon(\kappa t)^{3/2}c_p/Q$, the functional relation between Θ and R is represented as that between E and X or Z . These relations are to be verified by experiments.

Experiments

An $18.6 \times 5.9 \times 20.0$ cm fluid container was made of pyrex glass of which two 18.6×20.0 cm side walls were finished optically flat and fixed in parallel to each other. A small piece of electric heater made of tungsten filament was held 3 cm above the center of the bottom plate of container. For the test medium, pure water or mixture of glycerin and water was used keeping its temperature and mixing ratio uniform throughout in the container.

For Mach-Zehnder interferometry, a He-Ne gas laser light source was used. The block diagram of the system was shown in Fig. 3. As

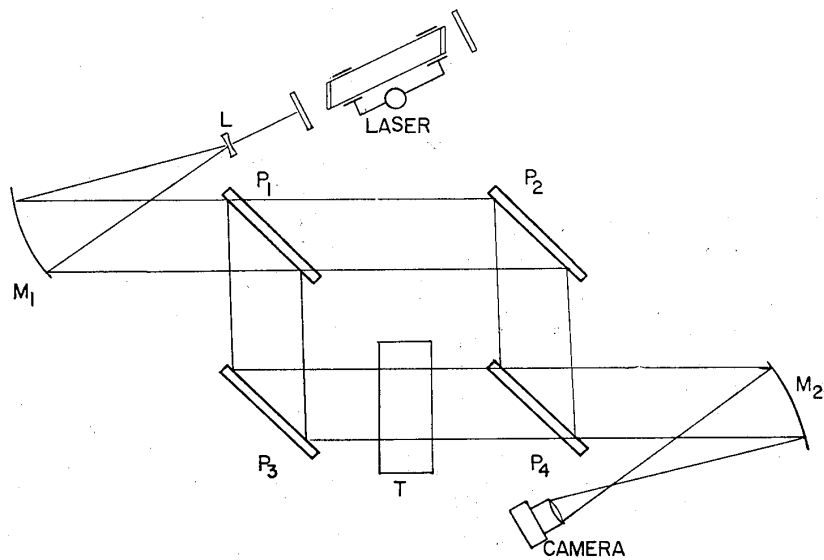


Fig. 3. Block diagram of experimental apparatus.

shown in the figure, a small diverging lens was inserted in front of the laser light source in order to illuminate the flow widely enough. The superiority of the gas laser as the light source of the interferometer has been ascertained by us (7), so it may be needless to mention here again. The photograph of the water container and the optical system was shown in the Fig. 4.

The instantaneous heat source was realized by applying the electric current to the tungsten filament for one second, and the amount of heat released was adjusted at any value by controlling the current. The interferograms of the flow field were taken at every

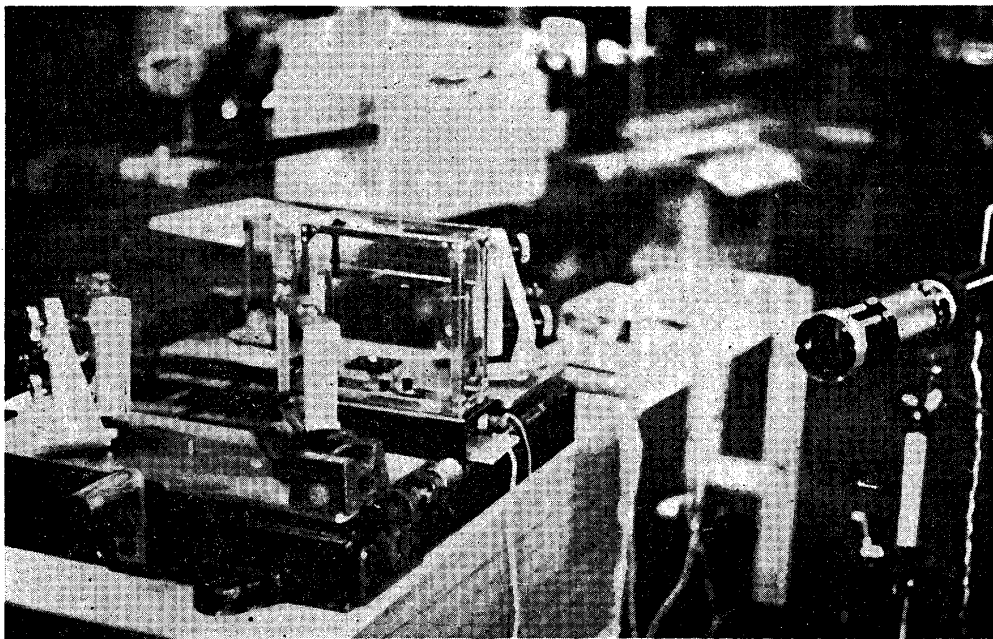
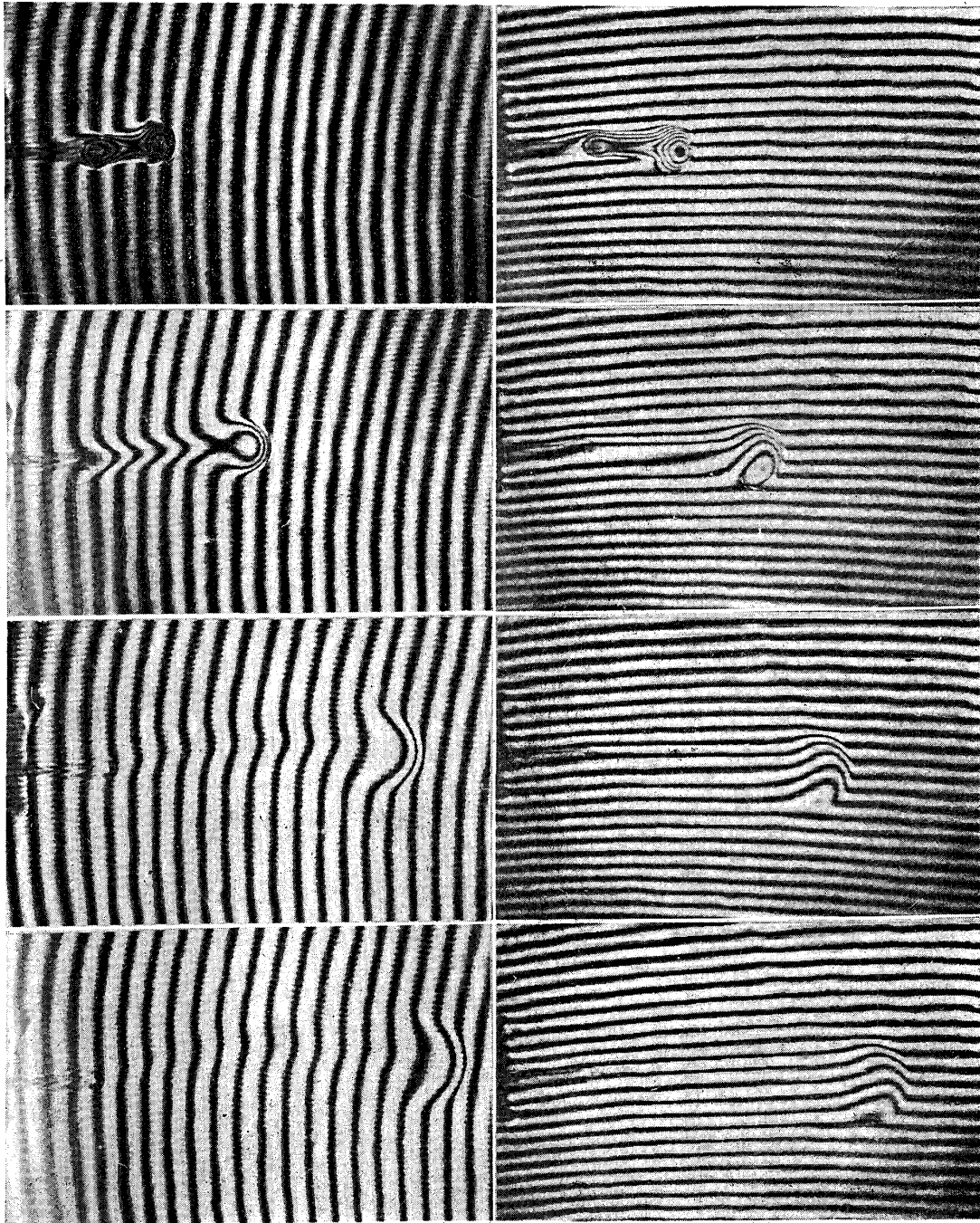


Fig. 4. Photograph of apparatus.

Fig. 5. Interferograms, vertical and horizontal fringe, $t = 2, 4, 6, 8$ sec.



two second after the heat released by a motor-driven camera. Two sets of the interferograms were taken for each experimental condition, one was those with vertical fringe pattern which were used to obtain the horizontal temperature distributions and the other was those with the horizontal pattern which are useful for analysis of the vertical temperature distributions. Fig. 5 shows a set of examples of these interferograms.

The experiments were carried out in pure water at three different temperatures of 17°C, 25°C and 30°C and in the mixture of glycerin and water with four kinds of mixing ratio of 10, 20, 30 and 40% glycerin in volume at 25°C. The amount of heat released at the source was adjusted to 0.15 cal in all the experiments.

Under these conditions, the parameters cover the range of $5 < \sigma < 30$, $80 < G < 700$.

Results and Discussions

The fringe shifts in each interferogram are measured for each case of the experiments. Figs. 6 to 9 show examples of the fringe shift distributions along the horizontal and vertical lines through the point of highest temperature in the sequence of the time for water and glycerin-water mixture, respectively. According to the suggestions of the self-similarity theory, these curves for all the experimental conditions should be compiled into a single curve by use of the similarity variable E and X or Z .^{*} They are shown in Figs. 10 and 11 for water and Figs. 12 and 13 for water and glycerin mixture. In Figs. 10 and 12, the approximation solutions for the initial stages, the Gaussian distribution is shown in the dotted line. From these curves, it may be concluded that the self-similarity has been verified experimentally in the temperature distribution along the horizontal axis. As for the distribution along the vertical axis, the evidence of similarity is less marked, probably due to accompanying wakes.

^{*} $E = \varepsilon(\kappa t)^{3/2} c_p$, that is $E = \theta K/Q$. Since K/Q is the same constant throughout our experiments, E is proportional to θ .

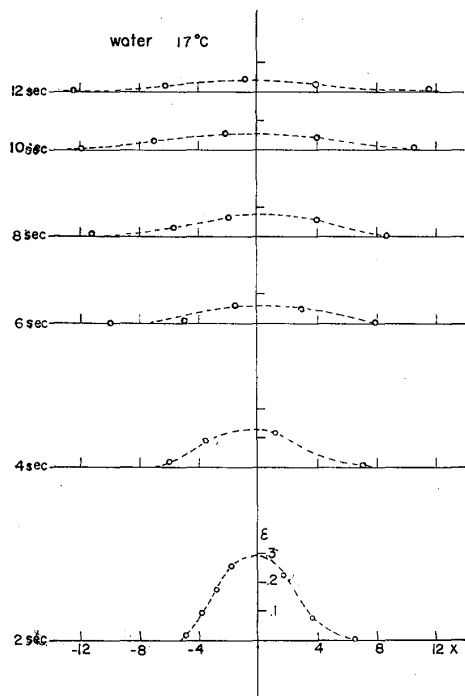


Fig. 6. Fringe shift distributions along the vertical line in water of 17°C, arbitrary scale.

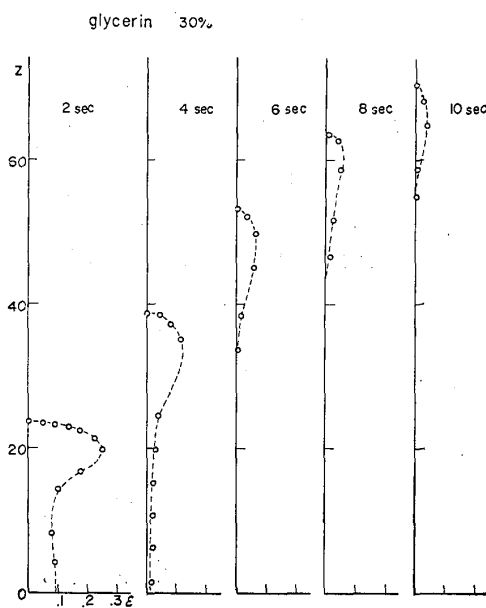


Fig. 7. Fringe shift distributions along the horizontal line in water of 17°C, arbitrary scale.

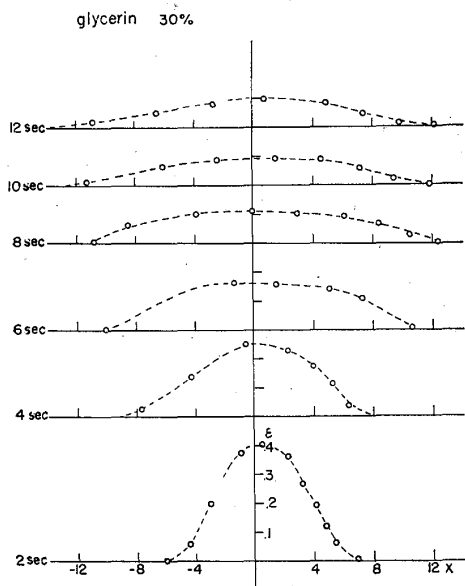


Fig. 8. Fringe shift distributions along the vertical line in 30% glycerin mixture, arbitrary scale.

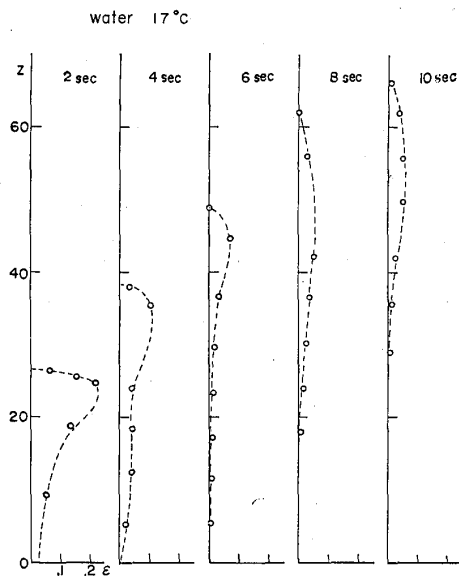


Fig. 9. Fringe shift distributions along the horizontal line in 30% glycerin mixture, arbitrary scale.

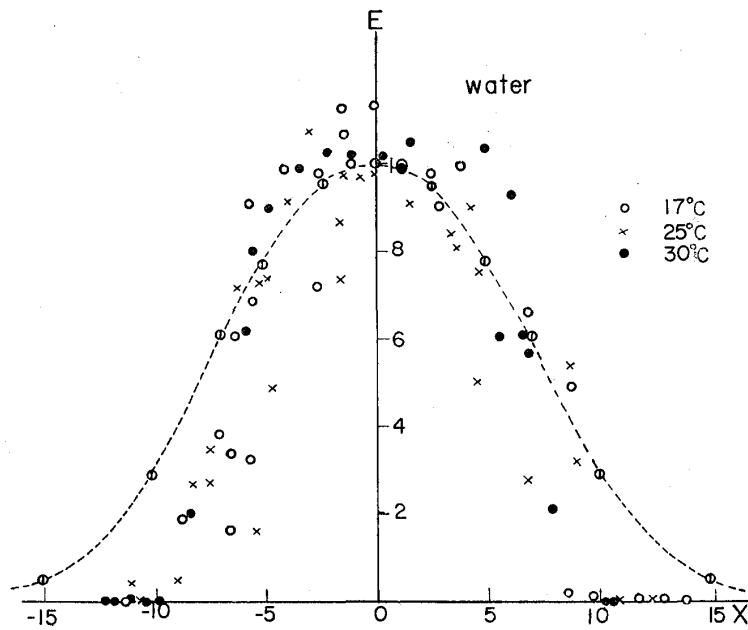


Fig. 10. The relation between E and X , water.

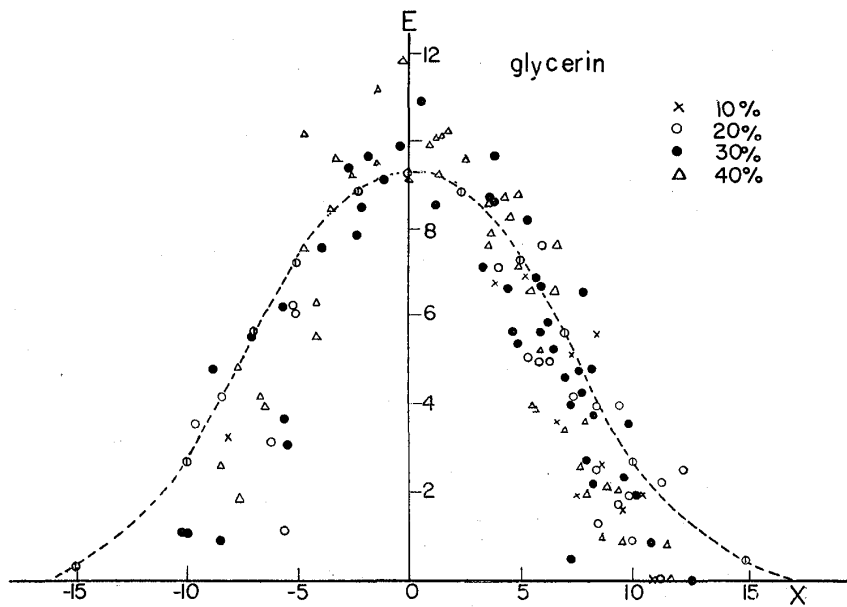


Fig. 12. The relation between E and X , glycerin mixture.

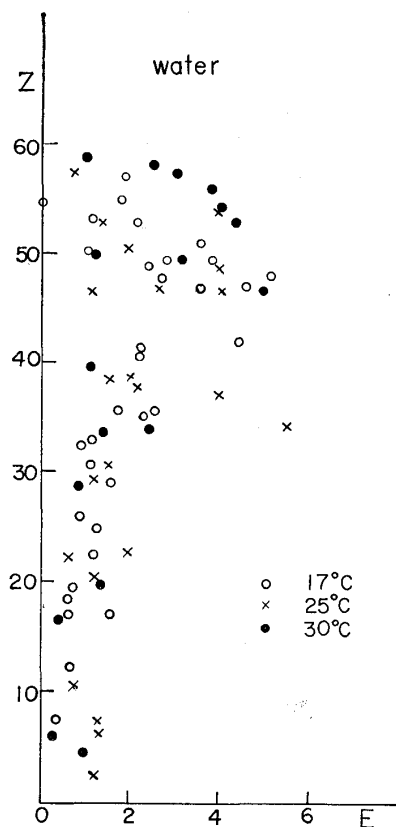


Fig. 11. The relation between E and Z , water.

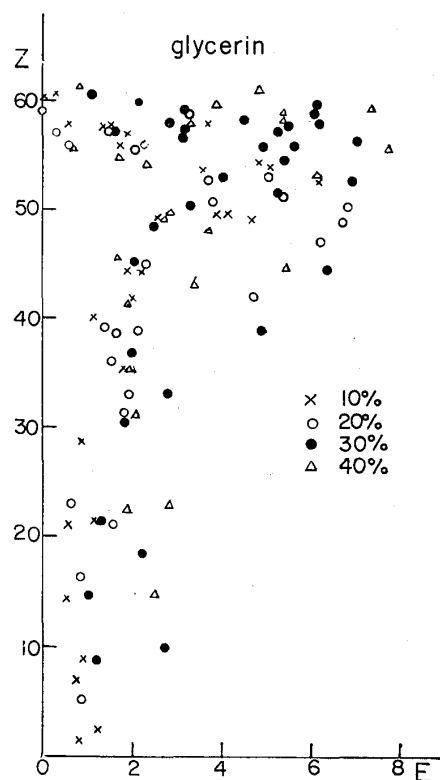


Fig. 13. The relation between E and Z , glycerin mixture.

Acknowledgements

The author wishes to express her cordial thanks to Professor S. Asaka for his useful advise and discussions during this work, and also many thanks due to Dr. K. Oshima for his encouragement. This work has been partly supported by the grant-in-aid for the fundamental scientific research from the Ministry of Education.

Reference

- 1) R. S. Scorer: J. Fluid Mech. 2 (1957) 583.
- 2) J. S. Turner: Proc. Roy. Soc. London A 239 (1957) 61.
- 3) J. S. Turner; J. Fluid Mech. 7 (1960) 419.
- 4) B. Woodward: Quart. J. R. Meteor. Sci. 86 (1959) 144.
- 5) B. R. Morton: J. Fluid Mech. 9 (1960) 107.
- 6) Y. Oshima. Nat. Sci. Rep. Ochanomizu Univ. 15-2 (1964) 65.
- 7) K. Oshima, K. Sugaya, M. Yamamoto, Y. Oshima: Bulletin Inst. Space Aero. Sci. Univ. Tokyo 1-1 (1965) (in Japanese).